
CASE REPORT

Atypical Langerhans Cell Histiocytosis: A Case Report

C Lo¹, WK Chan², G Lo³

¹*Department of Radiology, Queen Mary Hospital, Pokfulam, Hong Kong*

²*Department of Pathology, Hong Kong Sanatorium & Hospital, Happy Valley, Hong Kong*

³*Department of Radiology, Hong Kong Sanatorium & Hospital, Happy Valley, Hong Kong*

INTRODUCTION

Langerhans cell histiocytosis (LCH) is the most common dendritic cell disorder. It is named for the similarity of the lesional cells to the Langerhans cells found in the skin and mucosa. LCH can be divided into three forms based on number of lesions and systems involved.¹ The clinical manifestation of LCH depends on the number of sites and systems involved. Most (70%) cases of LCH are the unifocal (localised) form, which is limited to a single bone or few bones and may involve the lung. Patients with this form of LCH are usually aged 5 to 15 years. Another 20% of LCH cases are the multifocal unisystem (chronically recurring) form, which involves multiple locations in bones and the reticuloendothelial system (liver, spleen, lymph nodes and skin). This form is often accompanied by diabetes insipidus when pituitary gland is involved. Patients with this form of LCH are usually aged 1 to 5 years. The remaining 10% of cases of LCH are the multifocal multisystem (fulminant) form, which is often fatal. This form of LCH is characterised by disseminated involvement of the reticuloendothelial system with anaemia and thrombocytopenia. Patients with this form of LCH are usually aged 1 to 2 years. We present a case of atypical LCH and describe the pathological and radiographical features.

CASE REPORT

A boy, aged 2 years 10 months, presented with a rapidly enlarging right supraorbital soft tissue mass with inflammatory signs for 4 weeks. Plain film radiographs were not obtained, but magnetic resonance imaging (MRI) was ordered, to rule out orbital cellulitis or orbital tumour including rhabdomyosarcoma.

MRI scan showed a large expansile lytic lesion in the right orbital ridge. Multiple cortical breaks noted in the bone were associated with a soft tissue mass measuring 3.3 × 1.6 × 3.4 cm (transverse × anteroposterior × craniocaudal; Figure 1). This lesion was T1 isointense (Figure 2) and T2 heterogeneously hypointense with small T2 hyperintense foci (Figure 3). Marked enhancement of the soft tissue mass was noted after contrast injection (Figure 4). The orbital globe, extraocular muscles, lacrimal gland, optic nerve, and optic chiasm were normal.

Biopsy of the mass was then performed by an ophthalmologist. The biopsy results showed atypical LCH. *BRAF* mutation analysis was negative, indicating a low risk of recurrence.

Positron-emission tomography with MRI (PET-MRI)

Correspondence: Department of Radiology, Queen Mary Hospital, Pokfulam, Hong Kong.
Email: chrissy.lo@gmail.com

Submitted: 13 Aug 2017; Accepted: 11 Sep 2017.

Contributors: All authors designed the study, acquired and analysed the data, drafted the manuscript, and had critical revision of the manuscript for important intellectual content. All authors had full access to the data, contributed to the study, approved the final version for publication, and take responsibility for its accuracy and integrity.

Conflicts of Interest: All authors have disclosed no conflicts of interest.

Funding/Support: This case report received no specific grant from any funding agency in the public, commercial, or not-for-profit sectors.

Ethics Approval: Patient consent was waived by the ethics board (Ref REC-2019-16).

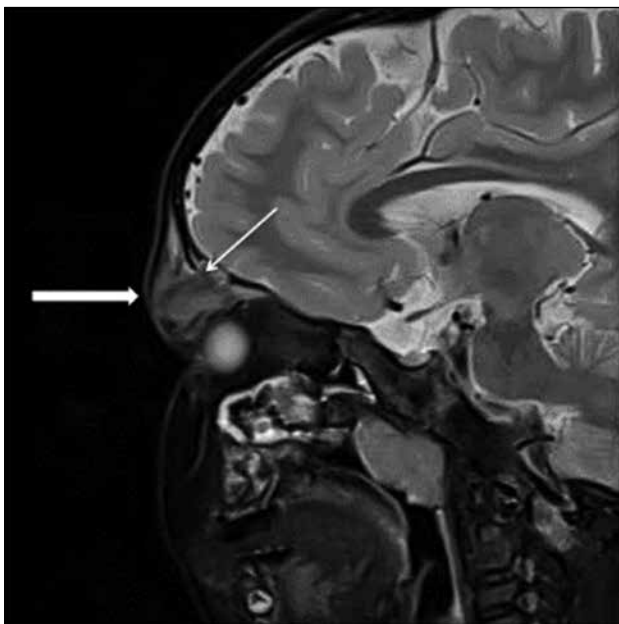


Figure 1. Magnetic resonance image showing large right supraorbital mass (thick arrow) with multiple cortical breaks (thin arrow).

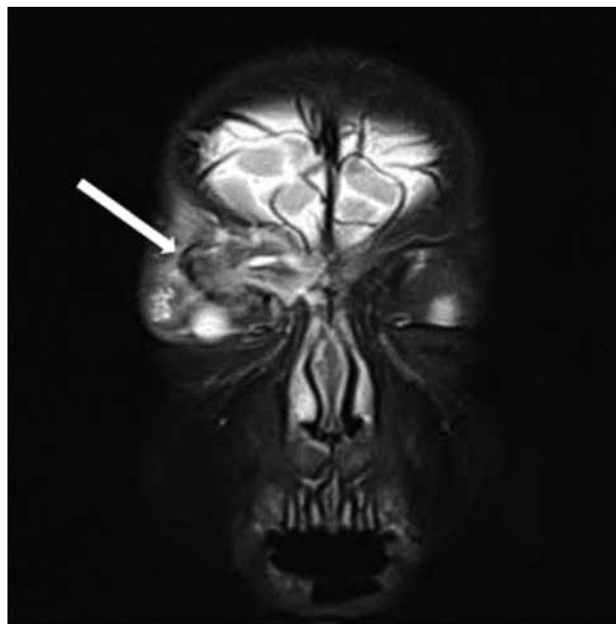


Figure 3. Magnetic resonance image showing T2-weighted heterogeneously hypointense right supraorbital mass (arrow).



Figure 2. Magnetic resonance image showing T1-weighted isointense right supraorbital mass (arrow).

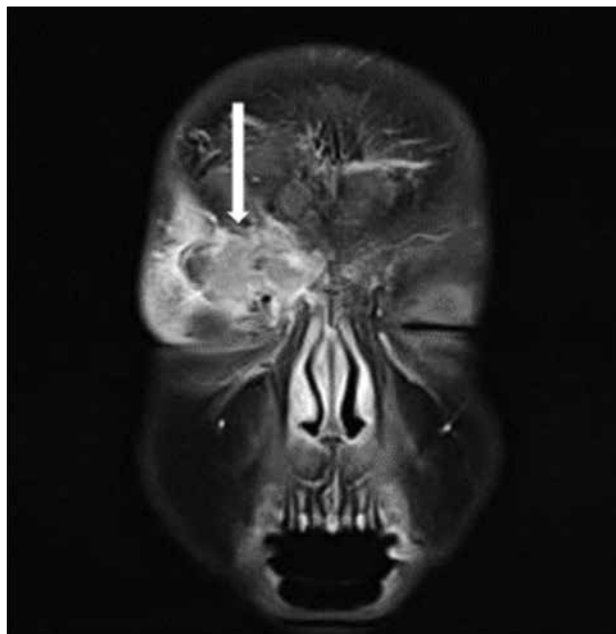


Figure 4. Post-contrast magnetic resonance image showing markedly enhancing right supraorbital mass (arrow).

was then chosen to evaluate the whole body because of the lower radiation dose reduction compared with PET-CT. PET-MRI scan showed the right orbital lesion to be hypermetabolic. SUVmax was 5.7 (Figure 5). No other hypermetabolic lesion was seen in the rest of

the body (Figure 6). As part of the PET-MRI protocol in our hospital, a complimentary low-dose computed tomography (CT) of the thorax was also obtained. The CT scan did not show any centrilobular nodules or lung cysts (Figure 7).

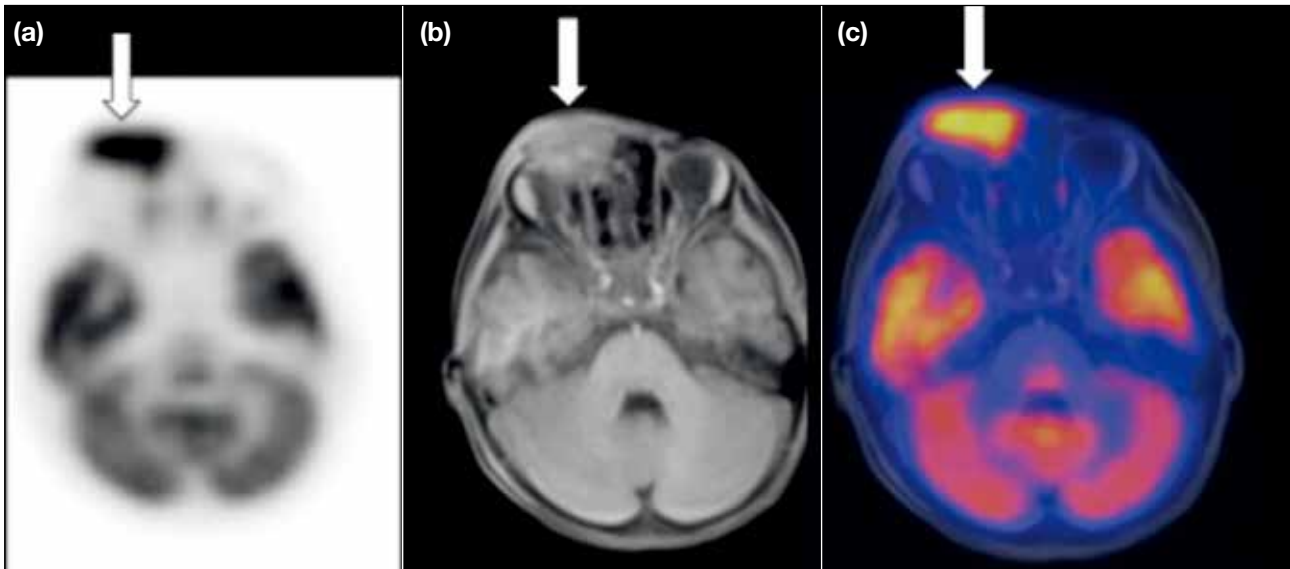


Figure 5. (a) Positron-emission tomography, (b) magnetic resonance imaging, and (c) positron-emission tomography magnetic resonance imaging showing hypermetabolic right supraorbital mass with SUVmax 5.7 (arrows).

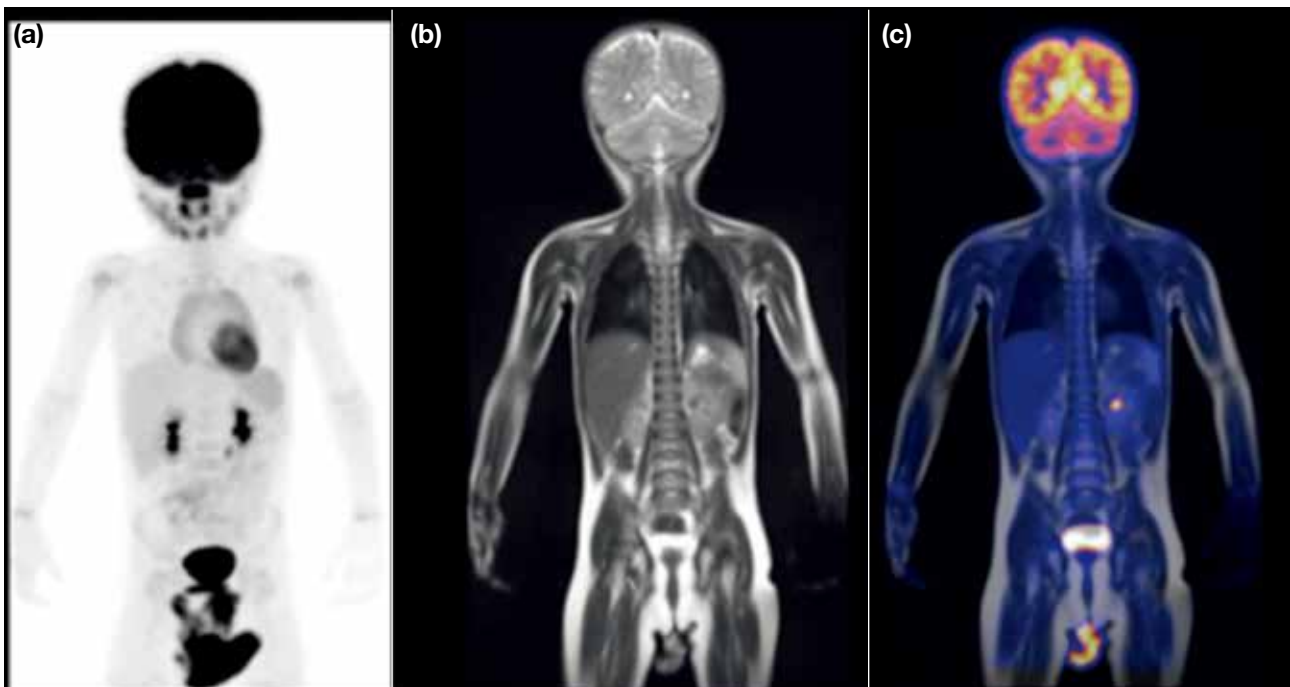


Figure 6. (a) Positron-emission tomography, (b) magnetic resonance imaging, and (c) positron-emission tomography magnetic resonance imaging showing absence of other hypermetabolic lesions in the rest of the body.

Because the supraorbital lesion was the only lesion and the prognosis was good, we decided that the patient would undergo surgery. However, surgery at this age may cause deformity. Therefore, the patient is now undergoing 6 months of chemotherapy to shrink the mass before surgery.

DISCUSSION

Radiology

Typical LCH lesions present with well-defined lytic lesions with bevelled edges in the skull.¹ MRI scan usually shows a soft tissue mass within the diploic space that is isointense on T1-weighted images, hyperintense



Figure 7. Low-dose computed tomography of the thorax showing normal lungs with no cystic lesions.

on T2-weighted images,^{1,2} and enhances after contrast injection.¹ Decreased T2 signal is seen in the healing phase.¹

In the present case, the isointense T1 images and the markedly enhancing post-contrast images are all consistent with LCH features. The atypical feature seen on the MRI scan was the presence of heterogeneous T2 low signal throughout the mass. In typical LCH cases, decreased T2 low signal indicates healing.¹

However, in the present case, PET-MRI showed hypermetabolic activity in the supraorbital mass, indicating active disease. SUVmax of the supraorbital mass was 5.7 (reference SUVmax of mediastinal blood pool: 0.61). The lesion was shown to be unifocal because the whole-body PET-MRI scan did not reveal any other tumours. This knowledge of the lesional activity helped us to manage this case.^{3,4} PET-MRI can also be used to monitor therapy.^{3,4}

A study that compared ¹⁸F-fluorodeoxyglucose (FDG)-PET with plain film radiographs, CT scans, MRI scans, and bone scans showed that, overall, FDG-PET was rated confirmatory or superior in 235 (92%) lesions out of 256.⁴ Whole-body FDG-PET can detect LCH activity and early response to therapy in bone and soft tissues with much greater accuracy than other conventional imaging modalities.⁴

Pathology

Histopathological examination of the incisional biopsy showed a plump mononuclear cell population with large lobulated nuclei, some with grooves and others with small central nucleoli. The cells showed moderately abundant pale to eosinophilic cytoplasm. Immunostaining results demonstrated positive staining for CD1a and langerin, confirming Langerhans cell origin. Because of the higher than usual mitotic count of up to 22 per 10 high power fields, and because there was some variation in nuclear size with some cells having distinct nucleoli, we diagnosed atypical LCH. The features were insufficient for a diagnosis of Langerhans cell sarcoma.

CONCLUSION

This case provided a unique opportunity to use PET-MRI to investigate metabolic activity of disease within the supraorbital mass and throughout the whole body. Using PET-MRI rather than PET-CT resulted in a radiation dose reduction of >50%.³ The choice of PET-MRI is especially appropriate for such a young patient, because he will need to have periodic follow-up scans for his disease.

REFERENCES

1. Zaveri J, La Q, Yarmish G, Neuman J. More than just Langerhans cell histiocytosis: a radiologic review of histiocytic disorders. *Radiographics*. 2014;34:2008-24. [Crossref](#)
2. Lim SJ, Lim MK, Park SW, Kim JE, Kim JH, Kim DH, et al. Langerhans cell histiocytosis in the skull: Comparison of MR image and other images. *JKSMRM*. 2009;13:74-80.
3. Kaste SC, Rodriguez-Galindo C, McCarville ME, Shulkin BL. PET-CT in pediatric Langerhans cell histiocytosis. *Pediatr Radiol*. 2007;37:615-22. [Crossref](#)
4. Phillips M, Allen C, Gerson P, McClain K. Comparison of FDG-PET scans to conventional radiography and bone scans in management of Langerhans cell histiocytosis. *Pediatr Blood Cancer*. 2009;52:97-101. [Crossref](#)